UNIVERSITY OF ZIELONA GÓRA

CIVIL AND ENVIRONMENTAL ENGINEERING REPORTS

E-ISSN 2450-8594

CEER 2025; 35 (2): 0222-0233
DOI: 10.59440/ceer/202032

Original Research Article

NUMERICAL SIMULATION OF UNCONFINED COMPRESSION TESTS OF SANDSTONE USING THE DISCRETE ELEMENT METHOD IN LS-DYNA

Mohammad Ashikur RAHMAN, Nur Syafiq Aiman NORDIN, Muhammad Irfan SHAHRIN[1], Rini Asnida ABDULLAH, Nor Zurairahetty Mohd YUNUS

Department of Geotechnics and Transportation Engineering, Faculty of Civil Engineering, Universiti Teknologi Malaysia, Johor Bahru, Malaysia

A b s t r a c t

This study presents a numerical simulation of unconfined compression tests (UCTs) on sandstone, utilizing the Discrete Element Method (DEM) in LS-DYNA. The primary objective of this research was to find an optimal mesh configuration to imitate the laboratory testing process by numerical modeling to enhance the reliability of data and reduce the time and cost required for complex experiments. Laboratory-derived rock properties were integrated into the DEM simulation as input parameters. Five numerical models were simulated with varying mesh densities to optimize mesh size. The results were validated by comparing failure mode, stress-strain curves, and uniaxial compressive strength (UCS) with experimental data. A model with a mesh size of 40/30 elements illustrated the closest correlation to the laboratory test, exhibiting a similar stress-strain curve pattern and a minimal UCS difference of 2.62%. Additionally, the failure modes observed in both simulations aligned closely. This similarity between the results of the laboratory experiment and the numerical model proves the efficiency of the numerical model in simulated laboratory tests and offers an opportunity to calibrate the micro-parameters of other constitutive models which can save both the time and money required to determine complex parameters, especially avoiding the risk of critical laboratory experiments.

Keywords: unconfined compression test, discrete element method, LS-DYNA software, mesh convergence, sandstone rock

1. INTRODUCTION

Physical testing in a laboratory or field can be expensive and time-consuming for several reasons such as the costs of equipment, personnel, supplies, and overhead. In the laboratory, the time required for testing can vary depending on factors such as the type of test being performed, the equipment used, the

[1] Corresponding author: Muhammad Irfan Shahrin: Department of Geotechnics and Transportation Engineering, Faculty of Civil Engineering, Universiti Teknologi Malaysia, Skudai, 81310, Johor, Malaysia, muhammadirfan.s@utm.my, +607 5531581

sample size, analysis of required data, and the need to calibrate and maintain equipment [1]. Due to the limitations of physical testing, numerical simulation has become a widespread practice to solve engineering problems. Numerical simulations help engineers optimize design, reduce development time, and minimize costs. The Discrete Element Method (DEM) is a powerful numerical simulation technique utilized to simulate the behavior of granular materials [2] and is widely used in engineering to model the rock.

This study sought to imitate the laboratory testing process with an optimum mesh size. Mesh convergence is crucial to ensure that the accuracy of numerically simulated results will not be affected by the mesh size across different projects. By identifying the optimal mesh density, unnecessary calculations associated with finer meshes can be avoided, thereby reducing simulation time [3]. Moreover, numerical simulation of laboratory tests can help calibrate the micro-parameters associated with the complex behavior of natural heterogeneous anisotropic material without facing the difficulties of conducting challenging laboratory tests [4].

Numerical simulation of an engineering problem involves representing the real-world problem in an abstract form for analysis and interpretation [5]. Different numerical simulations can be applied to address the same problem, depending on the chosen modeling approach. Conversely, the same numerical simulation can be used to solve a variety of distinct physical problems. Numerical simulation is a versatile tool that offers numerous benefits, enabling efficient exploration of different scenarios and conditions to determine the optimal solution [6]. Though in some cases numerical simulation can be ineffective due to complex data requirements and high computing efficiency [7], however, it is more cost-effective than physical testing, reducing the cost of product development and research [8]. Early numerical simulations of the Unconfined Compression Strength test used the Finite Element Method (FEM) to model rock behavior under axial loading [9]. Later, the Discrete Element Method (DEM) was introduced to capture fracture initiation and propagation more accurately [2]. The Particle Flow Code (PFC) further improved UCS test simulations by incorporating particle-based interactions [10]. Coupled FEM-DEM models enhanced realism by integrating continuum and discontinuum mechanics [11]. Recent advances include machine learning-assisted simulations for better prediction and efficiency [12]. Novel predictive models such as Genetic Algorithm (GA) [13], Adaptive Neuro-Fuzzy Inference System (ANFIS) [14], Artificial Neural Networks (ANN) [15], and Multivariate Adaptive Regression Splines (MARS) [16] have been developed using soft computing techniques. The performance of these models is evaluated using a range of statistical measures to assess their effectiveness [17, 18]. By utilizing advanced algorithms and computational tools, numerical simulations can deliver highly accurate results, enhancing our comprehension of intricate systems and processes. The failure mode behavior of rocks depends on the rock type. In numerical simulation methods such as Finite Element Analysis (FEA) or Computational Fluid Dynamics (CFD), the output result is significantly influenced by the mesh size [19]. It is crucial to carefully consider the appropriate mesh size and quality based on the physics of the problem, computational resources, and desired level of accuracy. Choosing an incorrect mesh size can cause inaccurate results, convergence issues, increased computational time, and misinterpretation of failure mechanisms, ultimately compromising the reliability and efficiency of the simulation [20].

Numerical simulation, particularly the Discrete Element Method (DEM), provides a cost-effective and efficient alternative to physical testing in rock engineering by optimizing mesh convergence, reducing computational costs, and accurately replicating laboratory experiments. An optimal mesh size in numerical simulations can accurately replicate laboratory test results while reducing computational time and costs, making numerical modeling a viable alternative to physical testing in rock engineering. Therefore, it is necessary to conduct a detailed study of the mesh convergence of sandstone to ensure the accuracy and reliability of the numerical modeling. This study

aims to identify the optimal mesh density to ensure simulation accuracy while minimizing unnecessary calculations, thereby enhancing the reliability of numerical models for rock behavior analysis.

2. METHODOLOGY

2.1. Research procedure

This research is comprised of three key parts, namely performing laboratory experiments, conducting numerical simulation, and validation of laboratory and numerical results. An Unconfined Compression Test (UCT) was conducted in the laboratory on a sandstone sample and numerical simulation was performed with variable mesh size. The stress-strain curve, maximum compressive strength and failure modes are crucial outputs from UCT used commonly to describe the mechanical behavior of the material [21]. Therefore, these parameters have been compared to identify the optimum mesh configuration as well as to validate the numerical model. Fig. 1 presents the flowchart of this work.

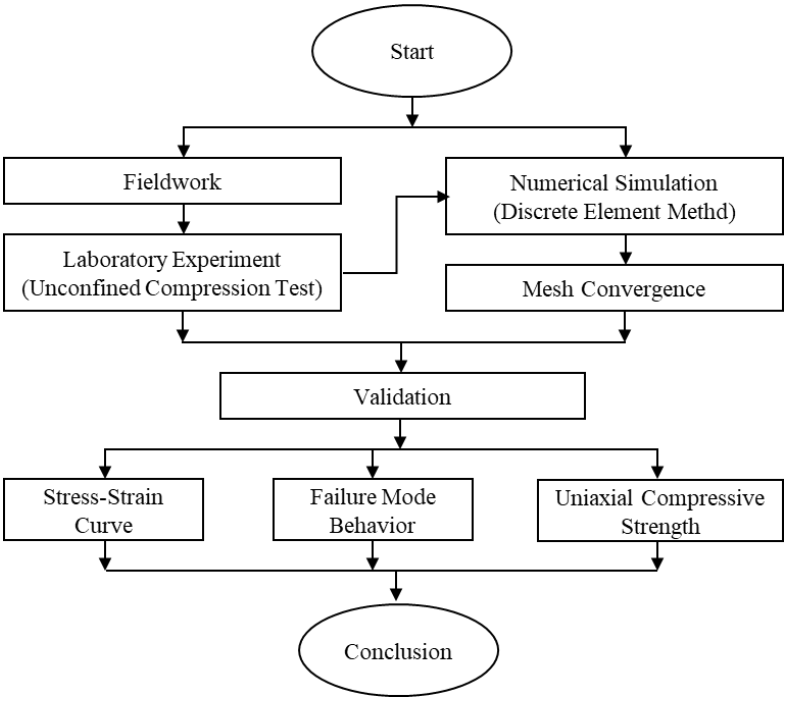

Fig. 1. A view of the Flowchart of numerical simulations

2.2. Laboratory experiment

Rock samples were collected from the Mersing area of Johor, Malaysia, the prominent geological unit is the Mersing formation. Unconfined compression test (UCT) was performed at the laboratory on these samples, and geomechanical properties of rock such as uniaxial compressive strength, maximum longitudinal strain, etc. were measured. Three cylindrical specimens were prepared having a length of 110 mm and a diameter of 50 mm, respectively. Fig. 2 shows the samples prepared for this test.

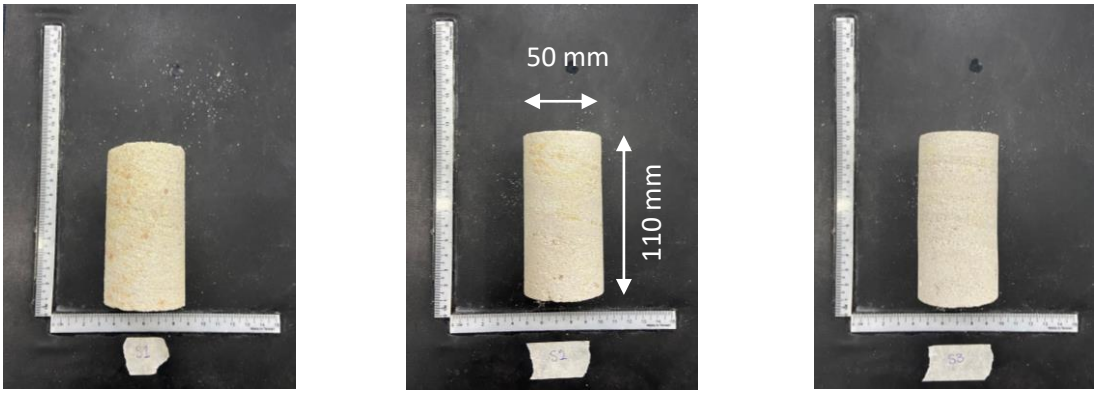

(a) Sample S1 (b) Sample S2 (c) Sample S3

Fig. 2. Samples used for UCT

From the test, the vertical displacement and horizontal dispacement were measured using a small dispalcement LVDT sensor (25 mm) and the encountered strain was plotted against the applied stress. From this graph, the above-mentioned geomechanical properties were obtained. Consequently, the failure mode of the sample was observed to judge the efficacy of the numerical analysis framework for simulating the fracture behavior of sandstone. The test set up is shown in Fig. 3.

Fig. 3. Test setup for UCT

2.3. Numerical analysis

Five numerical models were simulated using a parametric approach with variable mesh density. 8-noded elements were used to prepare the models and the number of elements in the circumferential direction (NECD) and the number of elements along the length of the cylinder (NELC) were systematically adjusted as shown in Table 1 to produce variable mesh densities [3]. These models were categorized by their NECD/NELC ratio, ranging from 100/75 (super fine mesh) to 10/7.5 (super coarse mesh). The numerical model coarse mesh is shown in Fig. 4.

Table 1. Mesh sizes considered in numerical modeling to study the convergence effect

Parameter	Super Fine Mesh (a)	Fine Mesh (b)	Normal Mesh (c)	Coarse Mesh (d)	Super Coarse Mesh (e)
Radius (mm)	25	25	25	25	25
Length (mm)	110	110	110	110	110
NECD[1]	100	60	40	20	10
NELC[2]	75	45	30	15	7.5

[1]NECD: Number of element circumferential direction
[2]NELC: Number of elements along the length of the cylinder

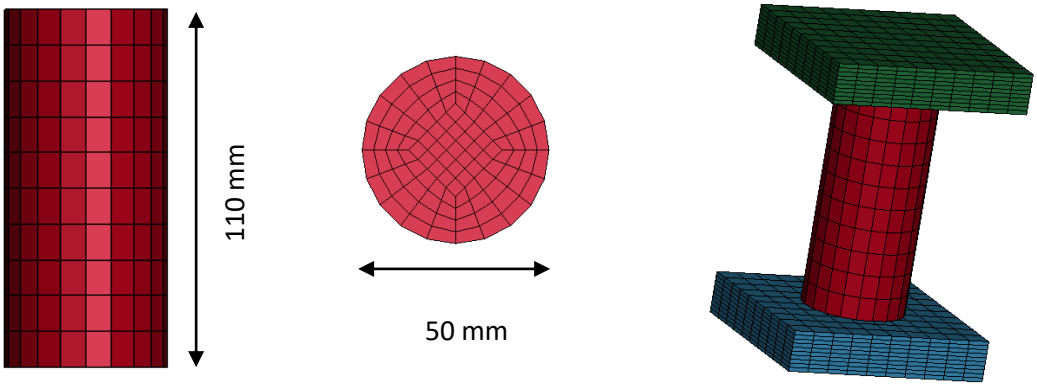

(a) Length of the specimen (b) Cross-section of the specimen (c) Numerical orientation for UCT

Fig. 4. Numerical model of the sample for Coarse mesh size

To mimic the test setup for UCT, a cylindrical rock sample was modeled between two steel plates. The steel plate on top and bottom of the sample was modeled as an elastic material. The rock mass was represented using the Bonded Particle Method (BPM) which was introduced by Potyondy and Cundall [10]. In this method, a densely packed model consists of non-uniform-sized circular (in two dimensions) or spheroidal-shaped (in three dimensions) particles bonded together by parallel bonds at the points of their contact. These bonds can experience tensile, bending, shear, and torsional force thus simulating the comprehensive mechanical behavior of solid mechanics, however independent of the DEM [22]. Calibrated micro-parameters were input into the DEM model [23] as tabulated in Table 2.

Table 2. Input micro-properties of UCT DEM model of sandstone (after Mardalizad, Scazzosi [23])

Properties	Value	Properties	Value
Density, RO (t/mm^3)[1]	2×10^{-9}	Post peak dilatancy decay, E_{drop}	1
Poisson's ratio, PR[1]	0.34	Three times the maximum aggregate diameter, LOC-WIDTH	1.35
Output selector for effective plastic strain, NOUT	2	Maximum shear failure surface parameter, A_o (MPa)[1]	-19.04
Unit conversion factor for length, RSIZE	0.03937	Maximum shear failure surface parameter, A_1 (MPa)	0.6529
Unit conversion factor for stress, UCF	145	Maximum shear failure surface parameter, A_2	0.00097
Compressive damage scaling parameter, B1	1.1	Initial yield surface cohesion, A_{0y} (MPa)	21.621
Tensile damage scaling exponent, B2	1.35	Initial yield surface coefficientA_{1y} (MPa)	1.11569
Damage scaling coefficient for triaxial tension, B3	1.15	Initial yield surface coefficient, A_{2y}	0.00251
Fractional dilatancy, ω	0.5	Residual failure surface coefficient, A_{1f} (MPa)	0.7563
λ-stretch factor, S_λ	100	Residual failure surface coefficient, A_{2f}	0.00097

[1] Data collected from laboratory experiment

From the numerical simulation of the UCT test for sandstone, the stress vs strain curve was generated for each model. From these curves, the maximum compressive strength was obtained. Additionally, the failure mode of the numerical model was observed. The findings from these numerical simulations were compared with laboratory test results to validate the numerical model. The mesh size of the best-performing numerical model was identified as the optimum configuration.

3. RESULTS AND DISCUSSION

3.1. Findings from the experimental test

The laboratory investigation found that the axial compressive strength of the sandstone varies from 8.21 MPa to 24.72 MPa while encountering a compressive strain within the limit of 1.8% to 2.2%. The observed fluctuations in estimated parameters can be attributed to several factors like rock heterogeneity, fineness grade of sandstone, loading direction, sample position relative to geological features [24], and differences between in situ and lab conditions. However, these findings align with the typical range for sandstone as found in the literature [25]. The stress-strain curve obtained from UCT is illustrated in Fig. 5.

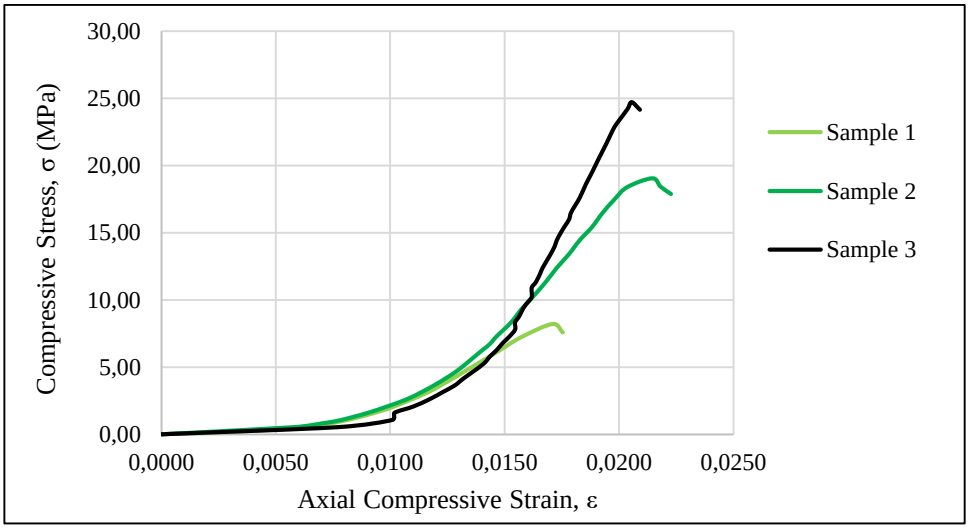

Fig. 5. Stress vs Strain curve obtained from UCT

The initial deformation includes grain rearrangement, pore collapse, and localized stress concentration at grain boundaries [26]. The intial strain was observed from the UCT conducted at the laboratory. Findings from the laboratory investigation have been summarized and tabulated in Table 3. Considering the shape of the graph and the value of parameters, Sample 2 was chosen as a representative sample and compared with numerical data.

Table 3. Summary of estimated geomechanical properties of sandstone from UCT

Sample ID	Unconfined Compressive Strength (MPa)	Axial Strain (mm/mm)
S1	8.21	0.0209
S2	**19.04**	**0.0223**
S3	24.72	0.0175

The observed failure mode from the laboratory experiment matches the typical mode of failure [27]. Sample 1 experienced a minor Y-shaped failure, double shear mode was observed for Sample -2 and Sample-3 demonstrated axial splitting where cracks were observed in the diagonal direction of the specimen. The following figure (Fig. 6) illustrates the comparison between the experimentally observed failure mode and the typical failure behavior of UCT.

Observed failure mode	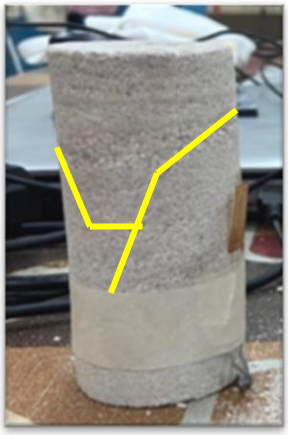		
Typical failure mode	Minor Y-shaped failure	Double shear failure	Axial Splitting
	(a) Sample 1	(b) Sample 2	(c) Sample 3

Fig. 6. Observed failure mode from laboratory experiment and typical failure behavior of UCT

3.2. Findings from numerical simulation

The stress vs strain curve was generated from the numerical models and presented in Fig. 7. The maximum compressive strength obtained from each numerical model is approximately 18.5 MPa, with values being consistent across all models except for the "Coarse Mesh" model. The mesh size significantly affected the stress distribution. Therefore different stress levels were concentrated on the nodes genereted by the varied mesh size mesh resulting in different failure modes. The "Coarse Mesh" model exhibited significantly higher strain, which is deemed unacceptable due to an anomaly in mesh convergence affecting the results. The minimum variation of strength was observed for the "Normal Mesh" model, exhibiting a difference of only 2.62% compared to experimental results. Antony, Olugbenga and Ozerkan [21] found a similar accuracy for maximum compressive strength from the numerical model with DEM. Therefore, the variation in the numerical model falls within the acceptable range.

Among the other models, the strain behavior varies widely. The "Super Fine Mesh" model demonstrated the ability to sustain larger strains (2.6%), whereas the "Fine Mesh" model exhibited limited deformation capacity (<1%). Both the "Normal Mesh" and "Super Coarse Mesh" models showed similar strain behavior (1.4%); however, the compressive strength was slightly higher (0.5%) for the "Normal Mesh" model, as illustrated in the stress-strain graph. The steep slopes of the stress-strain curves reflect the brittleness of the sandstone sample, indicating a sudden failure under stress without significant plastic deformation which is ideal for sandstone [28]. Since this numerical analysis framework cannot imitate the initial strain (as observed in laboratory test), the stress-strain curve from the numerical models do not match the experimental curve.

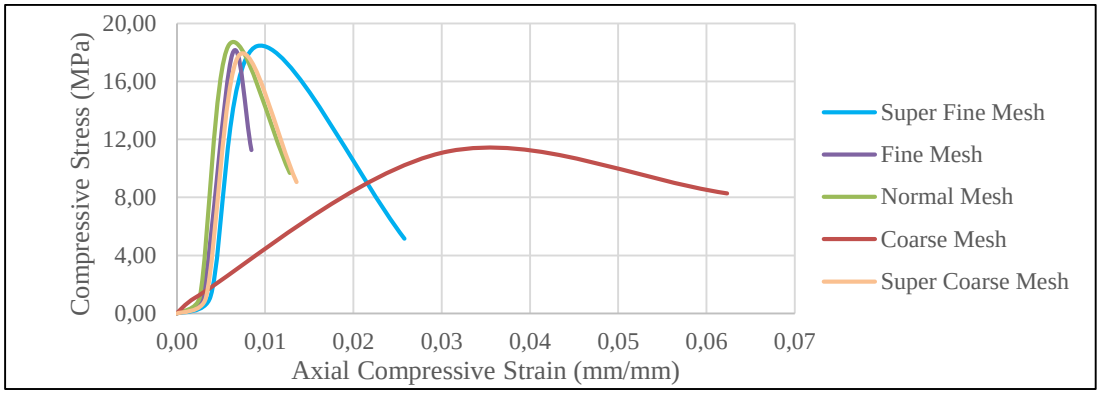

Fig. 7. Stress vs Strain curve generated from the numerical model with different mesh sizes

From the observation of failure mode shown in Fig. 8, the axial splitting mode was dominantly pronounced in models with "Super Fine Mesh", "Normal Mesh", and "Coarse Mesh". On the other hand, models with "Fine Mesh" and "Super Coarse Mesh" exhibited shearing failure along single-plane modes of failure behavior. It is clearly seen that the granular matrix of DEM particles can effectively reproduce the typical failure modes for UCT as similarity was observed between the physical test and numerical simulations.

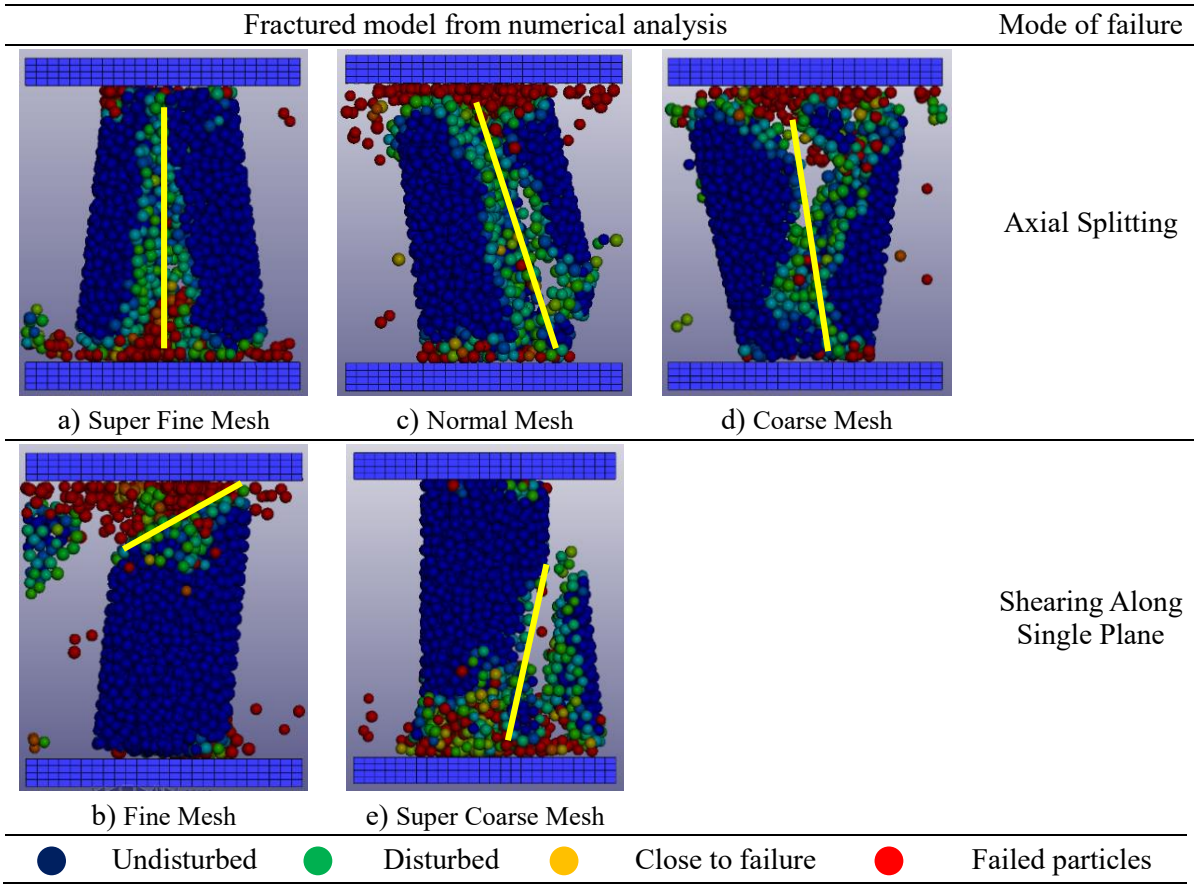

Fig. 8. Numerically simulated failure mode behavior in UCT

3.3. Validation of numerical model

To validate the numerical model, the estimated unconfined compressive strength, stress-strain relationship and failure mode were considered. Comparing the laboratory result and numerical simulation output, the strain obtained for the "Super Fine Mesh" model was closer to reality, but upon considering the longer time required to accomplish the numerical simulation, a normal size mesh was the optimum size to simulate the greatest level of strength.

Fig. 9 shows the comparison of uniaxial compressive strength of all numerical models and laboratory tests. The uniaxial compressive strength was found to be 19.04 MPa from the laboratory experiment. It can be seen that the "Normal Mesh" model is the most similar value of UCS with the laboratory test, which is 18.58 MPa. The percentage difference between laboratory tests and numerical results is 2.62%, which is less than 10% and is considered a good result. Though "Normal Mesh" and the "Super Coarse Mesh" model exhibited similar strength and strain, a larger mesh should be avoided considering the anamoly observed in the "Coarse Mesh" model.

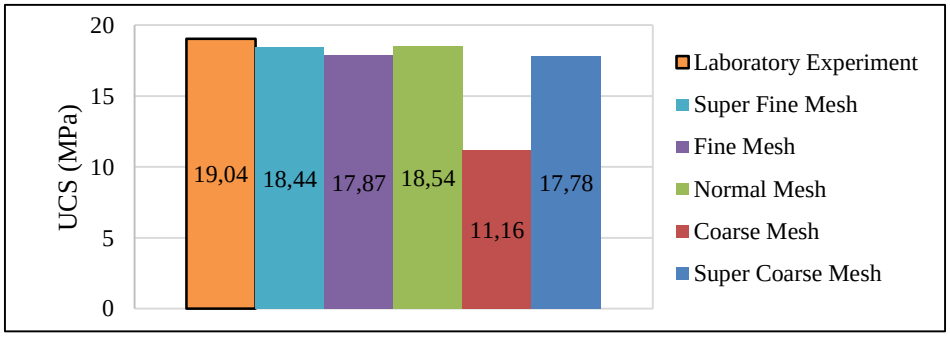

Fig. 9. Comparison UCS of UCT DEM model with the different mesh size

Furthermore, the failure mode observed from the physical test and numerical simulations aligns closely, which also validates the numerical model. Axial splitting was found to be the dominant failure mode for the sandstone sample which also aligns with the findings depicted in the literature [29]. Thereby, it can be stated that this analysis framework with the DEM model is suitable to simulate the behavior of sandstone.

4. CONCLUSION

This study employed the Discrete Element Method (DEM) to simulate an unconfined compression test (UCT) on sandstone rock, utilizing laboratory-derived rock properties as input parameters. By systematically varying mesh size, a 40/30 elements mesh configuration was identified as an optimal option to simulate the ultimate strength. The numerical simulation results demonstrated strong agreement with experimental data, exhibiting similar stress-strain curves, failure modes, and a minimal UCS difference of 2.62%. This mesh configuration is recommended for simulating sandstone behavior in engineering applications where strength is the primary concern, such as blast fragmentation. Conversely, for projects where strain is a critical parameter, such as stability and deformation monitoring in tunnel construction through sandstone, a "Super Fine Mesh" configuration of 10/7.5 elements is advised to ensure more reliable and detailed strain data. This study will enable engineers to choose optimum mesh sizes for numerical modeling of sandstone of Mersing formation. These findings establish the effectiveness of DEM as a valuable tool for replicating laboratory UCT, offering a more efficient and cost-effective approach for research in rock mechanics.

ACKNOWLEDGMENT

This research was funded by the Ministry of Higher Education (MOHE) through the Fundamental Research Grant Scheme (FRGS) under grant number FRGS/1/2022/TK06/UTM/02/53.

REFERENCES

1. Mahdi, DS and Alrazzaq, AAA 2023. Rock Mechanical Properties: A Review of Experimental Tests and Prediction Approaches. *Iraqi Journal of Oil and Gas Research* **3**, 106-115.
2. Cundall, PA and Strack, OD 1979. A discrete numerical model for granular assemblies. *Geotechnique* **29**, 47-65.
3. Shahrin, MI, Abdullah, RA, Alel, MNA, Saari, R, Ibrahim, NA, Yusof, NAM and Abd Rashid, MF 2021. Convergence Study for Rock Unconfined Compression Test Using Discrete Element Method. *International Journal of Integrated Engineering* **13**, 119-124.
4. Wu, Y, Hao, H, Gao, M, Gao, Z and Gao, Y 2023. A modified particle contact model for matching the ratios of uniaxial compressive to tensile strength of brittle rocks. *Geomechanics and Geophysics for Geo-Energy and Geo-Resources* **9**, 126.
5. Abhilasha, P and Antony Balan, T 2014. Numerical analysis of seepage in Embankment dams. *IOSR Journal of Mechanical and Civil Engineering* **4**, 13-23.
6. Wang, K-Y, Shallcross, DE, Hadjinicolaou, P and Giannakopoulos, C 2002. An efficient chemical systems modelling approach. *Environmental Modelling & Software* **17**, 731-745.
7. Biliński, T and Socha, T 2014. Numerical analysis of deflections of multi-layered beams. *Civil and Environmental Engineering Reports* **15**, 33-42.
8. Tahera, K, Earl, C and Claudia, E 2014. Integrating virtual and physical testing to accelerate the engineering product development process. *International Journal of Information Technology and Management* **13**, 154-175.
9. Zienkiewicz, OC and Cheung, Y 1968. *The finite element method in structural and continuum mechanics*.
10. Potyondy, DO and Cundall, PA 2004. A bonded-particle model for rock. *International Journal of Rock Mechanics and Mining Sciences* **41**, 1329-1364.
11. Mahabadi, O, Grasselli, G and Munjiza, A 2009. *Numerical modelling of a Brazilian Disc test of layered rocks using the combined finite-discrete element method*. RockEng09: 3rd Canada-US rock mechanics symposium.
12. Zhang, P, Yin, Z-Y and Jin, Y-F 2021. State-of-the-art review of machine learning applications in constitutive modeling of soils. *Archives of Computational Methods in Engineering* **28**, 3661-3686.
13. Shen, J and Jimenez, R 2018. Predicting the shear strength parameters of sandstone using genetic programming. *Bulletin of Engineering Geology and the Environment* **77**, 1647-1662.
14. Cao, W 2025. A comparative study of hybrid adaptive neuro-fuzzy inference systems to predict the unconfined compressive strength of rocks. *Journal of Engineering and Applied Science* **72**, 3.
15. Lawal, A, Adebayo, B, Afeni, T, Okewale, I, Ajaka, E, Amigun, J, Akinbinu, V and Apena, W 2024. Soft computing applications for optimum rock fragmentation: an advanced overview. *Geotechnical and Geological Engineering* **42**, 859-880.
16. Samui, P 2013. Multivariate adaptive regression spline (MARS) for prediction of elastic modulus of jointed rock mass. *Geotechnical and Geological Engineering* **31**, 249-253.
17. Armaghani, DJ, Amin, MFM, Yagiz, S, Faradonbeh, RS and Abdullah, RA 2016. Prediction of the uniaxial compressive strength of sandstone using various modeling techniques. *International Journal of Rock Mechanics and Mining Sciences* **85**, 174-186.

18. Koken, E and Strzalkowski, P 2024. Development of Soft Computing-Based Predictive Tools for Estimating the Young Modulus of Weak Rocks. *Civil and Environmental Engineering Reports* **34**, 182-193.
19. Devi, S, Nagaraja, K, Thanuja, L, Reddy, M and Ramakrishna, S 2022. Finite element analysis over transmission region of coronavirus in CFD analysis for the respiratory cough droplets. *Ain Shams Engineering Journal* **13**, 101766.
20. Lin, S, Zhang, C, Zhou, H and Dai, F 2020. Numerical analyses of mesh size effects on core discing. *Arabian Journal of Geosciences* **13**, 1-11.
21. Antony, S, Olugbenga, A and Ozerkan, N 2018. Sensing, measuring and modelling the mechanical properties of sandstone. *Rock Mechanics and Rock Engineering* **51**, 451-464.
22. Karajan, N, Han, Z, Ten, H and Wang, J 2013. *Interaction possibilities of bonded and loose particles in LS-DYNA*. Proceedings of the 9th European LS-DYNA Users' Conference, Manchester, UK.
23. Mardalizad, A, Scazzosi, R, Manes, A and Giglio, M 2018. Testing and numerical simulation of a medium strength rock material under unconfined compression loading. *Journal of Rock Mechanics and Geotechnical Engineering* **10**, 197-211.
24. Smolnik, G 2019. *DEM (PFC3D) numerical simulation of the influence of grain orientation on the strength of the Kimachi sandstone*. IOP Conference Series: Earth and Environmental Science **261**, 012047.
25. Moneey, R, Rahim, I and Musta, B 2022. *Some mechanical characterization of the Sandakan formation's sandstone, Sabah, Malaysia*. IOP Conference Series: Earth and Environmental Science **1103**, 012025.
26. Wong, T-f and Baud, P 2009. Grain crushing, pore collapse and strain localization in porous sandstone. *Mechanics of Natural Solids*, 239-254.
27. Basu, A, Mishra, D and Roychowdhury, K 2013. Rock failure modes under uniaxial compression, Brazilian, and point load tests. *Bulletin of Engineering Geology and the Environment* **72**, 457-475.
28. Noori, M, Khanlari, G, Sarfarazi, V, Rafiei, B, Nejati, HR and Schubert, W 2022. Experimental test and numerical simulation of the effect of brittleness on the microfracturing of sandstone. *Bulletin of Engineering Geology and the Environment* **81**, 309.
29. Fischer-Cripps, AC 2007. *Introduction to contact mechanics*. Springer.